Cellular Physiology and Biochemistry

Cell Physiol Biochem 2017;43:1346-1358
DOI: 10.1159/000481846
Published online: October 09, 2017
Accepted: June 13, 2017







**Original Paper**

# Protective Effects of Microrna-22 Against Endothelial Cell Injury by Targeting NLRP3 Through Suppression of the Inflammasome Signaling Pathway in a Rat Model of Coronary Heart Disease

Wei-Qiang Huang[a] Peng Wei[a] Ri-Qi Lin[a] Feng Huang[b]

[a]Department of Geriatric Cardiology, The First Affiliated Hospital of Guangxi Medical University, Nanning, [b]Department of Cardiology, The First Affiliated Hospital of Guangxi Medical University, Nanning, P.R. China

**Key Words**
Microrna-22 • NLRP3 • Inflammasome • Endothelial cells • Coronary heart disease • Signaling pathway • Apoptosis

**Abstract**
***Background/Aims:*** This study aimed to identify the role of microRNA-22 (miR-22) in endothelial cell (EC) injury in coronary heart disease (CHD) by targeting *NLRP3* through the inflammasome signaling pathway. ***Methods:*** A total of 24 healthy male Sprague-Dawley (SD) rats were divided into normal and atherosclerosis groups. The atherosclerosis rats were assigned into blank, negative control (NC), miR-22 mimic, miR-22 inhibitor and miR-22 inhibitor + siNLRP3 groups. A luciferase reporter gene assay was used to detect the relationship between miR-22 and NLRP3. MiR-22 expression as well as NLRP3 and caspase-1 mRNA and protein expression were measured using quantitative real-time polymerase chain reaction (qRT-PCR) and Western blotting. The activity and apoptosis of coronary arterial endothelial cells (CAECs) were determined by MTT and Hoechst 33258. CAEC lumen formation was detected by a lumen formation assay. An enzyme-linked immunosorbent assay (ELISA) was used to detect IL-1β, IL-6, IL-10 and IL-18 levels. ***Results:*** The results indicated that the atherosclerosis group significantly decreased miR-22 expression but increased NLRP3 and caspase-1 mRNA and protein expression. The cell survival rate was significantly increased in the miR-22 mimic group and significantly reduced in the miR-22 inhibitor group. The miR-22 mimic group displayed a lower apoptosis rate and more cells with obvious lumen walls and numerous tubular structures, while cells in the miR-22 inhibitor group were unable to form lumen walls and had a scattered distribution compared to the blank group. The ELISA showed that IL-1β, IL-6 and IL-18 levels were markedly decreased, while IL-10 was clearly increased in the miR-22 mimic group. In contrast, in the miR-22 inhibitor group, IL-1β, IL-6 and IL-18 levels were significantly increased, and IL-10 levels were decreased. ***Conclusion:*** Our findings

Dr. Feng Huang

Department of Cardiology, The First Affiliated Hospital of Guangxi Medical University, No. 6, Shuangyong Road, Nanning, Guangxi Zhuang Autonomous Region, (P.R. China)
Tel. +86-0771-5352770, E-Mail huangfeng3000@126.com

indicated that miR-22 could lower the levels of pro-inflammatory cytokines by inhibiting the NLRP3 inflammasome pathway, which suppresses CAEC apoptosis and protects CAECs in rats with CHD.



## Introduction

Coronary heart disease (CHD) as a common cardiovascular disease that mainly results from the build-up of atherosclerotic plaques, which narrows coronary arteries and decreases blood flow to the heart [1]. Although recent advances in early detection and therapies have been developed, CHD is still the major cause of sudden cardiac death and hospitalization around the world [2, 3]. According to statistics from 2012, 4.5% Asians over 18-years-old suffer from CHD, and the prevalence of this disease would increase by roughly 18% by 2030 [4]. Endothelial cell (EC) injury and inflammation have been largely implicated in the formation of coronary atherosclerosis [5, 6]. It is also well-established that microRNAs (miRNAs) participate in pathological processes in the cardiovascular system, such as endothelial dysfunction, inflammation, apoptosis, angiogenesis, and atherosclerosis [7, 8]. Therefore, it is possible that miRNAs may have a potential relationship with EC injury and inflammation in CHD.

MiRNAs are a class of small, endogenous, single-stranded non-coding RNAs that are approximately 22 nucleotides in length and can bind to messenger RNAs (mRNAs) to regulate the expression of target genes [9]. MiR-22 is located at chromosomal region 17p13.3 [10]. MiR-22 has been shown to be a tumor suppressor in metastatic breast cancer and gastric cancers [11, 12]. Interestingly, miR-22 expression has been found to be decreased in patients with coronary artery disease (CAD) and diseases displaying an inflammatory response [13]. Moreover, NLR family pyrin domain-containing 3 (NLRP3) coupled with downstream cytokines, including caspase-1, increased the severity of CHD and coronary atherosclerosis [14, 15]. Additionally, activation of NLRP3 leading to EC injury is considered a possible mechanism for explaining the deterioration in atherosclerosis [16]. Moreover, increasing evidence has demonstrated that targeting NLRP3 with small molecule inhibitors could potentially target inflammation [17]. For example, miR-223 negatively controls NLRP3 inflammasome activity [18]. However, no study has investigated whether miR-22 can regulate NLRP3. In this regard, it is hypothesized that there may be potential relationship between miR-22 expression and NLRP3 activation as well as EC injury in CHD. Therefore, the current study was conducted with the objective of identifying the role of miR-22 in NLRP3 activation and EC injury in rats with CHD.

## Materials and Methods

*Ethic statement*

This experiment was approved by the Ethics Committee of The First Affiliated Hospital of Guangxi Medical University and complied with the guidelines and principles of the Declaration of Helsinki.

*Experimental animals* A total of 24 healthy male Sprague-Dawley (SD) rats (3 ~ 4 months old), with a mean weight of 240 ± 60 g (animal certificate number: HNASLKJ20100330), were obtained from the Hunan SJA Laboratory Animal Co. Ltd. (Hunan, China). All the rats were kept in plastic cages with a stainless-steel cover (6 rats in each cage), and all rats were provided with free access to food and water (ordinary tap water) in an air conditioned room (25°C and 65% humidity). All the rats were acclimatized for one week to reduce the stress response caused by environmental changes.

*Model establishment and grouping*

The CHD models were created. Rats were divided into the normal and the atherosclerosis groups, with 12 rats in each group. After the rats were acclimatized for one week, rats in the normal group received a basic diet and tap water, while the atherosclerosis group received a high-fat diet containing 2% cholesterol,

0.5% sodium cholate, 3% lard oil, 0.2% propylthiouracil and 94.3% basic diet with vitamin D3 ($1.25 \times 10^6$ μ/kg). At the beginning of experiment, the right lower extremities of the rats in the atherosclerosis group were injected with vitamin D3 every 30 days (weighted $3 \times 10^6$ μ/kg).

*Detection of serum lipids and calcium levels*

At 3 months after the experiment, an intraperitoneal injection of sodium pentobarbital was used as anesthesia after the rats were fasted overnight. After the abdominal aorta was isolated, a pair of scissors was used to cut the abdominal aorta from the renal artery joints, and a needle was inserted, followed by the insertion of an injector for arterial blood collection. The specimens were centrifuged at 500 × g for 5 min to isolate the plasma. Then, the isolated plasma (1 ml) was used to detect the serum lipid and calcium levels. The total cholesterol (TC), triglycerides (TG), high-density lipoprotein cholesterol (HDLC), low-density lipoprotein cholesterol (LDLC) and $Ca^{2+}$ levels were measured using an Abbott Aeroset TM analyzer (Abbott Laboratories, Chicago, USA). The experiments were performed in triplicate to calculate the mean values.

*Oil red-O staining*

Coronary artery endothelial cells (CAECs) from the bottom of the coronary artery (approximately 1 cm) were immediately fixed for 10 ~ 15 min using 10% formalin. Then, distilled water was used to wash away the fixative solution. Thereafter, the cells were washed twice with 60% isopropanol and incubated with oil red-O staining solution for 15 min. Next, the cells were washed three times with 60% isopropanol and twice with distilled water. A microscope was used for the cell analysis and to photograph the stained cells.

*CAEC isolation, culture and identification*

The coronary artery near the heart was obtained and immersed in phosphate-buffered saline (PBS) and heparin for 5 min to prevent blood coagulation. The coronary artery was washed with PBS three times under sterile conditions and then immersed in 75% alcohol for 15 s. Subsequently, the coronary artery was cut into tissue fragments (1 $mm^3$) using a pair of ophthalmic scissors. The fragments were combined with 0.2% collagenase type II (3 ml) in a water bath at 37°C for 6 min and with 0.25% pancreatin (3 ml) in a water bath at 37°C for 5 min for digestion. The digestion was terminated via the addition of 3 ml Dulbecco's Modified Eagle's Medium (DMEM) supplemented with 10% fetal calf serum. After the supernatant was discarded, the cells were re-suspended in complete medium and incubated at 37°C in a humidified incubator with 5% $CO_2$. The culture medium was changed after 6 h and the non-adherent cells were removed. After the cells reached 80% confluence, thec culture medium discarded and the cells were washed with PBS three times. Then, 0.25% trypsin and 0.02% ethylene diamine tetraacetic acid (EDTA) were added to the culture flask. After oscillation, the trypsin solution was prompted to flow onto cell surface. The culture flask was then observed under a microscope. When most of cells displayed a round shape, culture medium supplemented with 10% fetal calf serum was immediately added to terminate the digestion. The cells were pipetted to remove the cell wall. After the cell suspension was absorbed, the cells were centrifuged, re-suspended in complete medium and mixed evenly. After adjusting then to the proper density, the cells were sub-cultured and cultured at 37°C in a humidified incubator with 5% $CO_2$ and the culture medium was changed every 3 days. After immunocytochemistry analysis, the cells were washed with PBS and incubated overnight with primary antibody. The following day, the cells were washed with PBS three times and incubated with second antibody at 37°C for 30 min. Finally, the cells were stained with diaminobenzidine (DAB) solution and observed and recorded 24-h culture.

*Cell transfection and grouping*

CAECs to be treated were incubated with homocysteine (HCY, 0.25 mmol/l) for 24 h and then the CHD models were established. The DNA Oligo for miR-22 over-expression was synthesized based on the target sequence that effectively promotes miR-22 expression to make double-stranded DNA. The pGCSIL-GFP vector was double digested with Age I and EcoR I, and then connected and transformed with double-stranded DNA. The positive clones were filtered by qRT-PCR. The plasmid was extracted and confirmed by restriction enzyme digestion and sequencing. MiR-22 over-expression (miR-22 mimic), inhibited expression of miR-22 (miR-22 inhibitor), and inhibitor of NLRP3 (siNLRP3) were synthesized and packaged in liposomes. The third generation of CAECs was transfected when cells reached 80% confluence. Liposomes

diluted to an appropriate proportion were added to the cell culture medium for co-culture for 24 h. The cells were grouped into the blank (cell without transfection), negative control (NC, transfected with irrelevant sequences), miR-22 mimic (transfected with miR-22 mimic), miR-22 inhibitor (transfected with miR-22 inhibitor), and miR-22 inhibitor + siNLRP3 (transfected with miR-22 inhibitor and siNLRP3) groups.

*Luciferase reporter gene assay*

MicroRNA.org was used to predict the relationship between miR-22 and NLRP3 and the miR-22 binding site in the NLRP3 3'-UTR. Sequences from the NLRP3 3'-UTR promoter region containing a coding site for miR-22 were generated to construct the NLRP3 3'-UTR-WT plasmid. Then, the binding site was mutated to construct the NLRP3 3'-UTR -MUT plasmid according to the instructions in the Plasmid Isolation Kit (Promega, Madison, WI, USA). Next, 293T cells in logarithmic growth phase were inoculated in 96-well plates until cells reached 70% confluence. Then, the cells were transfected with Lipofectamine 2000. The NLRP3-3'UTR-WT plasmid and miR-22 mimic plasmid were thoroughly mixed and co-transfected into the 293T cells. Meanwhile, NLRP3-3'-UTR-WT + NC (control group), NLRP3-3'-UTR-MUT + NC and NLRP3-3'-UTR-MUT + miR-22 mimics were respectively transfected into 293T cells. After incubation for 6 h, 293T cells were cultured for 48 h with 10% FBS, and luciferase activity was measured by chemiluminescence. The experiment was performed in triplicate, and the mean value was calculated.

*qRT-PCR*

Total RNA was isolated using a Trizol-based miRNA isolation protocol (Invitrogen, Carlsbad, CA, USA), which was then confirmed using a formaldehyde denaturing gel electrophoresis and ultraviolet-visible spectrometer. The reverse transcription of RNA (l μg) was performed with Avian myeloblastosis virus (AMV) Reverse Transcriptase to prepare cDNA. PCR primers were designed and synthesized by Invitrogen and are presented in Table 1. The PCR was conducted based on following conditions: (1) pre-denaturation at 94°C for 5 min; (2) followed by 40 cycles of denaturation at 94°C for 40 s, annealing at 60°C for 40 s, and extension at 72°C for 1 min; and (3) overlap extension at 72°C for 10 min. The products were separated by agarose gel electrophoresis. The PCR results were analyzed using the Opticon Monitor 3 software (Bio-Rad, Inc., Hercules, CA, USA). The threshold cycle (CT) was obtained by manually selecting the lowest threshold value in the amplification curve rising in parallel. The data were analyzed using the comparative CT method, which was defined as $2^{-\Delta\Delta Ct}$ to express the relationship for target gene expression between the experiment and control groups, where $\Delta\Delta CT = [CT(\text{target gene}) - CT(\beta\text{-actin})]_{\text{experiment group}} - [CT(\text{target gene}) - CT(\beta\text{-actin})]_{\text{control group}}$. The experiments were performed in triplicate to calculate the mean values. β-actin was used as an internal control.

*Western blotting*

Proteins from rat myocardial tissues and cells were extracted. Protein concentrations were measured using a BCA protein assay kit (Wuhan Boster Biological Technology Co., Ltd., Wuhan, China). Total protein was added to loading buffer and boiled at 95°C for 10 min. A total of 30 μg total protein was placed in each well. Proteins were separated by 10% polyacrylamide gel electrophoresis. During the electrophoresis, the separation voltage was initially 80 V, and then increased to 120 V. Wet transfer with a transfer voltage of 100 mV and a transfer time of 45 ~ 70 min was used to the proteins from the gel to the membrane. Membrane transfer was conducted with a polyvinylidene fluoride (PVDF), which was then incubated with 5% bovine serum albumin (BSA) for 1 h at room temperature. The proteins were identified via incubation with the rabbit anti-mouse NLPR3 (1:1000) and caspase-1 (1:1000) primary antibodies purchased from Cell Signaling Technology (MD, USA) and the anti-mouse β-actin (1:3000) primary antibody

**Table 1.** Primer sequences for qRT-PCR, qRT-PCR, quantitative real-time polymerase chain reaction; miR-22, microRNA-22; F, forward; R, reverse

| Gene | Sequences |
|---|---|
| miR-22 | F: 5'-ACAGTTCTTCAACTGGCAGCTT-3'<br>R: 5'-AAGCTGCCAGTTGAAGAACTGT-3' |
| NLRP3 | F: 5'- CTTCCTTTCCAGTTTGCTGC-3'<br>R: 5'- TCTCGCAGTCCACTTCCTTT-3' |
| caspase-1 | F: 5'-GCCCAAGTTTGAAGGACAAA -3'<br>R: 5'-GGTGTGGAAGAGCAGAAAGC-3' |
| β-actin | F: 5'- GTCAGGTCATCACTATCGGCAAT-3'<br>R: 5'- AGAGGTCTTTACGGATGTCAACGT-3' |

purchased from Becton, Dickinson and Company (BD, NY, USA) at 4°C overnight. Then, the membranes were rinsed with TBST 3 times for 5 min each. After incubation with goat anti-rabbit second antibody (MT-Bio, Shanghai, China) for 1 h at room temperature, followed by 3 additional membrane washes with TBST for 5 min each, the proteins were detected by enhanced chemiluminescence and quantified using a Bio-Rad Gel Doc EZ Imager (Bio-Rad, Inc., Hercules, CA, USA). β-actin was used as the internal control. The target bands were used to analyze gray values using the ImageJ software. The experiment was performed in triplicate to calculate the mean values.

*MTT assay*

The 2nd-3rd CAEC cell suspensions were diluted and inoculated at a density of $5 \times 10^4$ cells per well in 96-well plates. Six parallel wells were set up for each group. Cell grouping was performed when cells reached 80% confluence. After reoxygenation, 20 μl of MTT (Sigma, USA) were added to each well, which was incubated for 4 h at 37°C. After the MTT solution was removed, 150 μl of dimethyl sulfoxide (DMSO) were added to the wells in the plate, which was shaken for 10 min. The optical density (OD) of each well was measured at the wavelength of 490 nm using a microplate reader. Each sample was repeated in triplicate to obtain the mean OD values. The cell survival rate was calculated with the following equations: Cell survival rate = (OD value of experimental group – OD value of blank group) / OD value of blank group.

*Hoechst 33258 staining*

Cells in logarithmic growth phase were digested with 0.25% trypsin and 0.02% EDTA. After centrifugation, the cells were re-suspended in complete solution and inoculated in 500 μl at a density of $6 \times 10^5$ cell/well in 24-well plates at 37°C and 5% $CO_2$. After cells had completely adhered to the surface, cells on cover glasses were washed three times and then fixed with 4% paraformaldehyde for 15 min, followed by washing with PBS three times for 5 min each. The cells were stained with Hoechst 33258 solution for 15 min at 25°C, rinsed with distilled water and dried. The number of cells was observed under an inverted fluorescence microscope and five high-expression sights were randomly selected. Cells displaying pyknosis, condensation and light cell nuclei were regarded as apoptotic. The number of positive cells was recorded. The apoptosis rate is equal to the ratio of the number of positive cells to the total number of cells. Each experiment was processed three times to calculate the mean values.

*Lumen formation assay*

Matrigel (BD, #356230, 5 ml/vial) was routinely stored at -20°C. On the day before the experiment, the Matrigel was stored in a refrigerator at -4°C overnight to slowly melt it into a liquid state. The micropipettes (2 ml) and 24-well plates were pre-cooled on ice. Matrigel (500 μl) was added to each well and the 24-well plates were uniformly coated with Matrigel to prevent air bubbles by shaking. This entire experiment was performed on ice. The Matrigel was solidified in an incubator at 37°C for 30 min. Single cell suspension were digested and collected. In each well, cells were incubated with cell suspension (500 μl) at the density of $2 \times 10^5$ cells/ml. The treatments for each group were repeated multiple times. After the cells were incubated at 37°C for 4 h, 6 h and 15 h, the formation of lumen structures were observed with a microscope. Three randomly selected fields of view were photographed. The number of lumen structures was counted and the average number in each group was taken as the value. Each experiment was processed three times to obtain the mean values.

*Enzyme-linked immunosorbent assay* (*ELISA)*

Cells in the logarithmic growth phase were digested with 0.25% trypsin and 0.02% EDTA. After centrifugation, the cells were re-suspended in complete culture medium. Cell inoculation in 500 μl at a density of $6 \times 10^5$ cell/well was conducted in 24-well plates at 37°C with 5% $CO_2$ for 24 h. When the cells no longer adhered to the surface, they were centrifuged at 3000 × g for 10 min to remove the deposition and collect the cell supernatant. The cells were added to the plates (3 wells per sample, 100 μl/well) according to the instructions for the ELISA Kit (Boster Biological Technology Co., Ltd., Wuhan, China). The plates were incubated, washed and developed with TMB. A microplate reader was used to determine the absorbance values (A value) at 450 nm and OD values for IL-1β, IL-6, IL-10 and IL-18. The rest supernatants were stored at -20°C. A standard curve was drawn with the OD values on the ordinate axis and standard concentrations on the abscissa axis. The corresponding concentrations were found on the standard curve with the OD values. Each experiment was repeated three times to obtain the mean values.

*Statistical analysis*

Data analyses were performed using the SPSS 21.0 software (SPSS 21.0, SPSS Inc., Chicago, IL, USA). The count data were expressed as the case or rate. The quantitative data were shown as the means ± standard deviation (SD). The *t* test was applied for comparisons between two groups. One-way analysis of variance (ANOVA) was applied for multi-group comparisons (Homogeneity of variance test was adopted before analysis). The Least Significant Difference (LSD)-*t* was used to test pairwise comparisons among groups. A value of $P < 0.05$ was considered statistically significant.

**Table 2.** Comparisons of serum lipid and calcium levels of rats in each group (mmol/L), TC, total cholesterol; TG, triglyceride; LDLC, low-density lipoprotein cholesterol; HDLC, high-density lipoprotein cholesterol; *, compared with normal group, P < 0.05

| Group | TC | TG | LDLC | HDLC | $Ca^{2+}$ |
|---|---|---|---|---|---|
| Normal group | 4.19 ± 0.25 | 1.09 ± 0.21 | 1.01 ± 0.18 | 2.35 ± 0.20 | 2.66 ± 0.29 |
| Atherosclerosis group | 15.38 ± 0.56* | 4.04 ± 0.16* | 6.01 ± 0.32* | 2.41 ± 0.27 | 3.34 ± 0.34* |

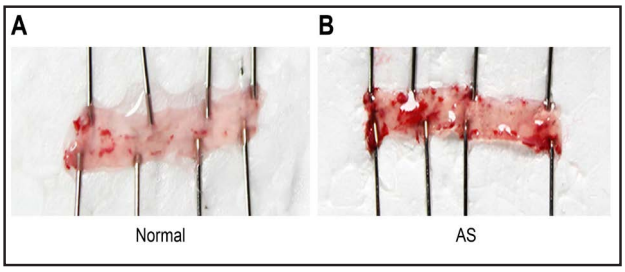


**Fig. 1.** Microscope images of the coronary artery (× 100).AS, atherosclerosis.

## Results

*Serum lipid and calcium levels between the normal and atherosclerosis groups*

The serum lipid and calcium levels indicated that the TC, TG, and LDLC levels and $Ca^{2+}$ concentration were significantly increased in the atherosclerosis group (all $P < 0.05$) compared with the normal group. No significant change was observed in the serum HDLC level between the two groups ($P > 0.05$) (Table 2).

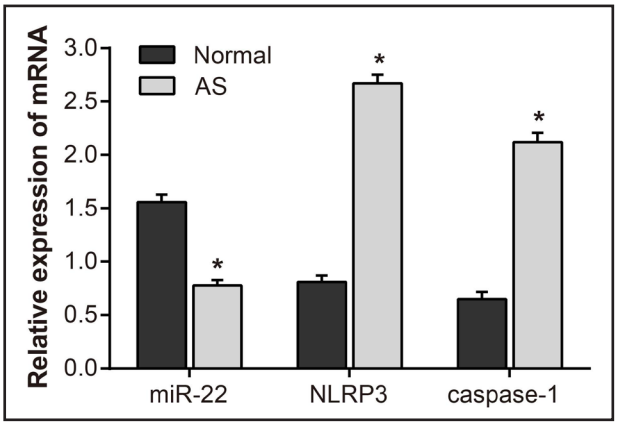


**Fig. 2.** MiR-22, NLRP3 and caspase-1 RNA expression in cardiac tissues between the normal and atherosclerosis groups. *, P<0.05 compared with the normal group; miR-22, microRNA-22; and NLRP3, nucleotide-binding domain and leucine-rich repeat protein 3.

*Morphological changes in the coronary arteries from rats in the normal and atherosclerosis groups*

The coronary arteries from each group were stained with oil red-O. The results showed that typical and mature atherosclerosis plaques appeared only in the atherosclerosis group, while no apparent atherosclerosis plaques were detected in the normal group (Fig. 1).

*miR-22, NLRP3, and caspase-1 RNA expression in myocardial tissues from the normal and atherosclerosis groups*

qRT-PCR was used to measure miR-22, NLRP3, and caspase-1 RNA expression in the myocardial tissues from each group. The results suggested a significant difference between the normal and atherosclerosis group ($P < 0.05$). Compared to the normal group, miR-22 expression was remarkably decreased, and NLRP3 and caspase-1 expression were significantly increased in the atherosclerosis group (all $P < 0.05$) (Fig. 2).

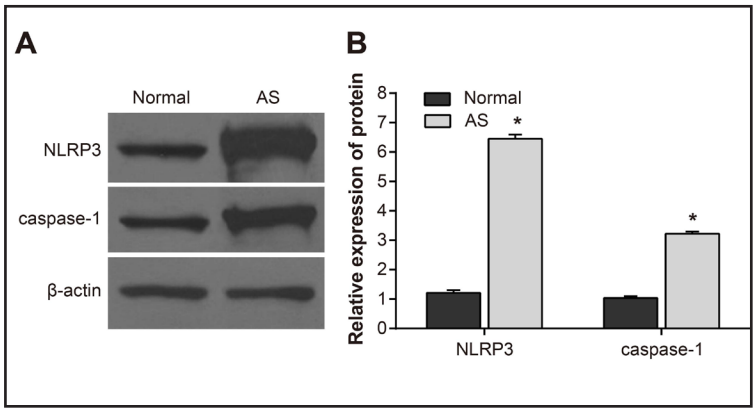


**Fig. 3.** NLRP3 and caspase-1 expression in myocardial tissues between the normal and atherosclerosis groups. (A) Western blotting images for NLRP3 and caspase-1. (B) NLRP3 and caspase-1 expression between the normal and the atherosclerosis group. *, P<0.05 compared with the normal group and NLRP3, nucleotide-binding domain and leucine-rich repeat protein 3.

*NLRP3 and caspase-1 protein expression in myocardial tissues from the normal and atherosclerosis groups*

Western blotting was used to examine NLRP3 and caspase-1 protein expression in myocardial tissues. The results indicated a significant difference between the normal and atherosclerosis groups ($P < 0.05$). Compared with the normal group, NLRP3 and caspase-1 protein expression were remarkably up-regulated in the atherosclerosis group (both $P < 0.05$) (Fig. 3).

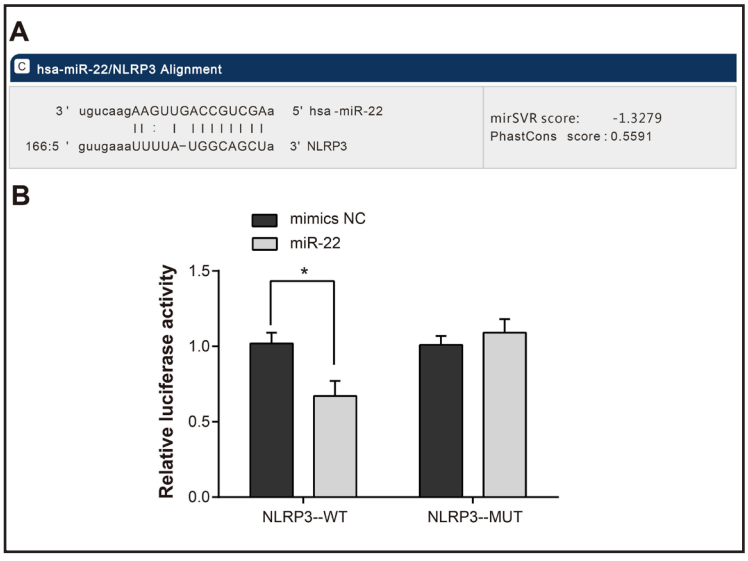


**Fig. 4.** The relationship between miR-22 and NLRP3. (A) The relationship between miR-22 and NLRP3 detected by bioinformatics software. (B) Verification of the luciferase activity results. *, P<0.05 compared with the normal group and NLRP3, nucleotide-binding domain and leucine-rich repeat protein 3.

*The relationship between NLRP3 and miR-22*

Microrna.org detected that NLRP3 is a miR-22 target gene (Fig. 4A). Thus, the NLRP3-3′-UTR-WT and miR-22 mimic plasmids were co-transfected into 293T cells. The luciferase activity in the NLRP3-3′-UTR-WT + miR-22 mimic group was remarkably decreased compared to the NLRP3-3′UTR-WT + NC group ($P < 0.05$). Additionally, no significant differences were observed when comparing the luciferase activities between the NLRP3-3′-UTR-MUT + NC and NLRP3-3′-UTR-MUT + miR-22 mimic groups ($P > 0.05$) (Fig. 4B).

*Observation and identification of morphological changes in CAECs*

The primary CAECs were observed with an inverted microscope after culturing for 24 h. The CAECs grew into a cobblestone-like monolayer and were small, short and spindle-shaped. The CAECs had a high diopter. The number of adherent cells was enhanced with the increasing number of culturing days. The spindle-shaped cells began to stretch and adhered to the wall. The cells developed into polygons or spindles until cultured for 5 - 7 days (Fig. 5). Three to four hours after cell passaging, the cells had become fusion. The morphologies of the passaged cells were identical to the primary cells and similar to a typical stone pavement.

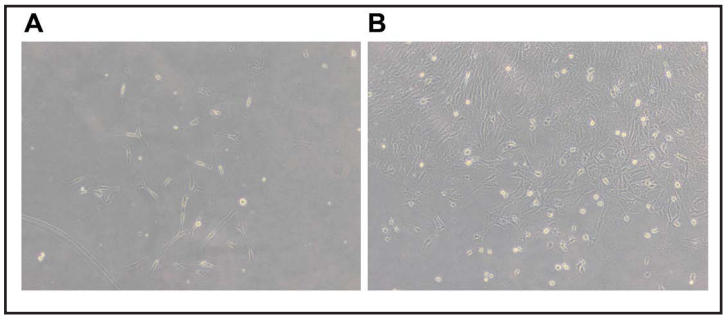


**Fig. 5.** CAEC morphological observations. (A) CAEC morphology at 24 h. (B) CAEC morphology on the 7th day (× 200). CAECs, coronary artery endothelial cells.

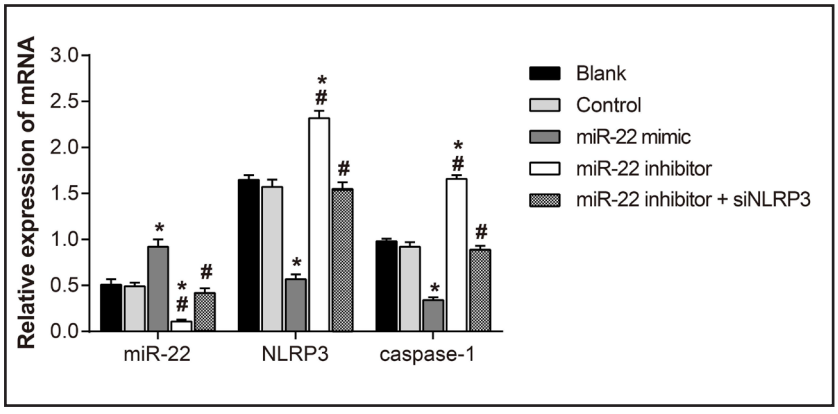


**Fig. 6.** MiR-22, NLRP3 and caspase-1 RNA expression in the groups measured by qRT-PCR. *, P<0.05 compared with the blank group; #, P<0.05 compared with the miR-22 mimic group; and NLRP3, nucleotide-binding domain and leucine-rich repeat protein 3.

According to the immunocytochemistry results, specific molecular markers of CAECs, including CD34, CD105, and Tie-2, were strongly positive; CD31 and vW were also positive.

*NLRP3, caspase-1 and miR-22 RNA expression in the CAECs groups*

Based on the qRT-PCR results and compared with the blank group, the expression of miR-22 in the miR-22 mimic group was markedly increased, while the expression of miR-22 decreased in the miR-22 inhibitor group. The miR-22 inhibitor group displayed significantly increased NLRP3 and caspase-1 mRNA expression, although the expression of those genes was decreased in the miR-22 mimic group compared with the blank group (all $P < 0.05$). There were no significant differences found between the blank, NC, and miR-22 inhibitor + siNLRP3 groups (all $P > 0.05$) (Fig. 6).

*NLRP3 and caspase-1 protein expression in the CAEC groups*

NLRP3 and caspase-1 protein expression were measured in the CAECs by Western blotting. The findings indicated that compared with the blank group, the miR-22 mimics group displayed remarkably decreased NLRP3 and caspase-1 expression levels, but their expression was significantly increased in the miR-22 inhibitor group (all $P < 0.05$). No significant differences were observed between the blank, NC, and miR-22 inhibitor + siNLRP3 groups (all $P > 0.05$) (Fig. 7).

*Cell survival rate in the CAEC groups*

MTT was used to measure the cell survival rate of the CAECs. Compared with the blank group, the cell survival rate of the miR-22 mimic group was remarkably increased, while that of the miR-22 inhibitor group was significantly decreased (both $P < 0.05$). There were no significant differences in the cell survival between the blank, NC and miR-22 inhibitor + siNLRP3 groups (all $P > 0.05$) (Fig. 8).

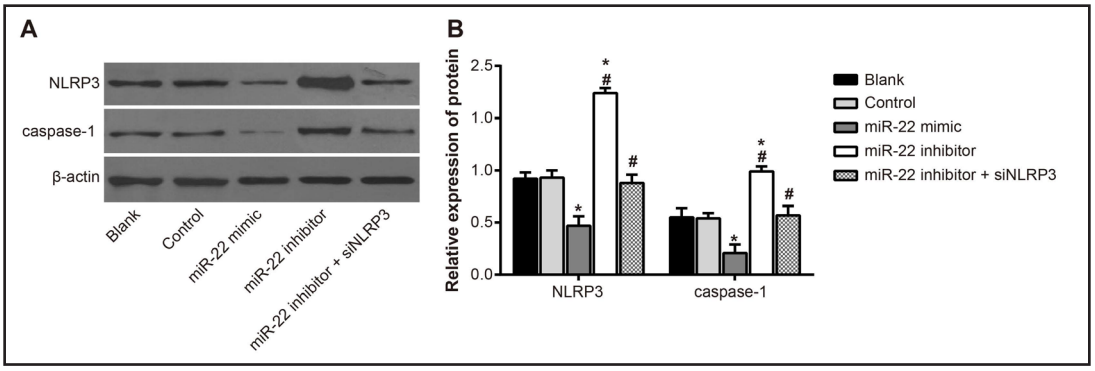


**Fig. 7.** NLRP3 and caspase-1 protein expression in the groups measured by Western blotting. (A) Western blotting images for NLRP3 and caspase-1. (B) NLRP3 and caspase-1 expression in each group. *, P<0.05 compared with the blank group; #, P<0.05 compared with the miR-22 mimic group; ad NLRP3, nucleotide-binding domain and leucine-rich repeat protein 3.

**Fig. 8.** CAEC cell survival rate in the groups measured by MTT. *, P<0.05 compared with the blank group; #, P<0.05 compared with the miR-22 mimic group; NLRP3, nucleotide-binding domain and leucine-rich repeat protein 3; and CAECs, coronary artery endothelial cells.

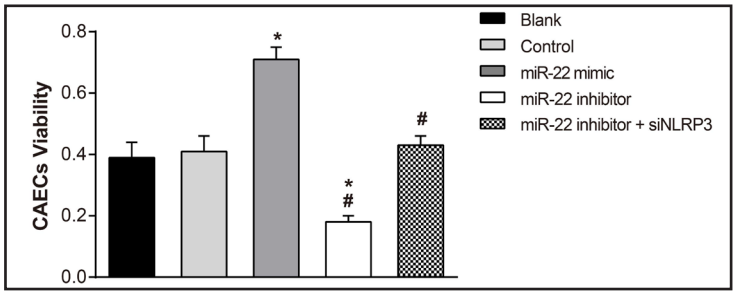


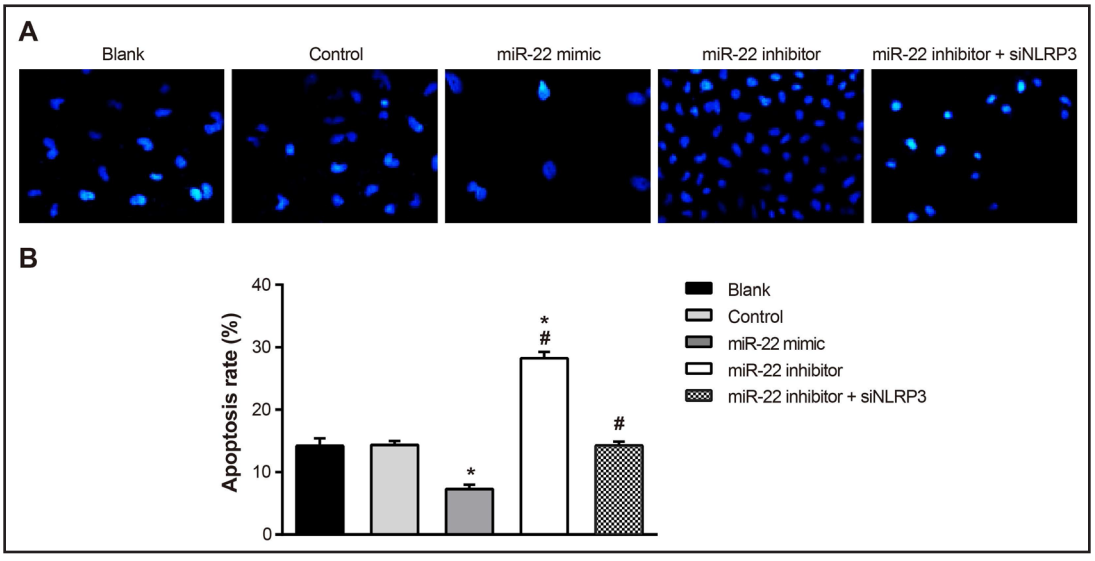


**Fig. 9.** CAEC apoptosis in the groups determined by Hoechst 33258 staining. (A) CAEC apoptosis in each group (× 200). (B) CAEC apoptosis rates in each group; *, P<0.05 compared with the blank group; #, P<0.05 compared with the miR-22 mimic group; NLRP3, nucleotide-binding domain and leucine-rich repeat protein 3; and CAECs, coronary artery endothelial cells.

*nCell apoptosis in the CAEC groups*

The results from the Hoechst 33258 staining indicated that CAECs were characterized by karyopyknosis, nuclear/chromatin condensation and the presence of apoptotic bodies in response to CHD. There were no significant differences found between the blank and NC

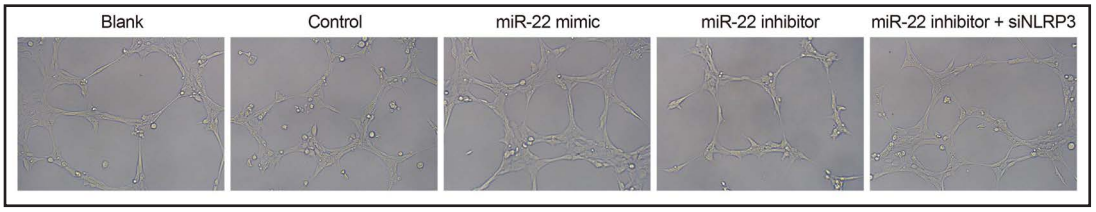


**Fig. 10.** Lumen formation conditions in the CAEC groups (× 200). NLRP3, nucleotide-binding domain and leucine-rich repeat protein 3 and CAECs, coronary artery endothelial cells.

**Table 3.** Comparisons of expressions of inflammatory factors (IL-1β, IL-6, IL-18 and IL-10) of rats in each group (pg/mL), *, compared with blank group, P < 0.05; #, compared with miR-22 mimic group, P < 0.05; miR-22, microRNA-22; IL, interleukin; NLRP3, nucleotide-binding domain and leucine-rich repeat protein 3

| Group | IL-1β | IL-6 | IL-10 | IL-18 |
|---|---|---|---|---|
| Blank group | 9.12 ± 0.37 | 43.14 ± 4.86 | 50.32 ± 3.75 | 79.36 ± 5.05 |
| Negative control group | 9.18 ± 0.89 | 42.88 ± 4.14 | 50.18 ± 4.21 | 78.85 ± 4.77 |
| miR-22 mimic group | 3.57 ± 0.22* | 21.54 ± 2.49* | 79.63 ± 4.66* | 23.47 ± 2.19* |
| miR-22 inhibitor group | 17.34 ± 1.73*# | 84.33 ± 5.25*# | 21.49 ± 3.15*# | 184.65 ± 4.32*# |
| miR-22 inhibitor + siNLRP3 group | 9.11 ± 0.62 | 43.05 ± 4.84 | 49.88 ± 3.96 | 79.42 ± 3.98 |

groups ($P > 0.05$). Compared with the blank group, the number of cells with incomplete nuclei was significantly reduced, and the apoptosis rate was decreased in the miR-22 mimic group (all $P < 0.05$). However, compared with the blank group, the miR-22 inhibitor group displayed significantly increased apoptotic cells, cells with incomplete nuclei and apoptosis rate (all $P < 0.05$). No significant differences were observed regarding the apoptosis rate between the miR-22 inhibitor + siNLRP3, blank and NC groups ($P > 0.05$) (Fig. 9).

*Lumen formation in the CAECs groups*

Although CAECs under CHD stress still possessed lumen-forming abilities, the lumens were few in number and displayed thin walls. Compared with the blank group, obvious lumens and numerous tubular structures were formed by CAECs in the miR-22 mimic group, while cells in the miR-22 inhibitor group were almost unable to form lumens, displaying a scattered distribution instead ($P < 0.05$). No significant differences were found in lumen-forming abilities of the blank, NC, and miR-22 inhibitor + siNLRP3 groups ($P > 0.05$) (Fig. 10).

*Inflammatory cytokine (IL-1β, IL-6, IL-10 and IL-18) levels among the groups*

ELISA was applied to measure the levels of inflammatory cytokines. Compared with the blank and NC groups, IL-1β, IL-6 and IL-18 levels were markedly decreased, while IL-10 levels were significantly increased in the miR-22 mimic group (all $P < 0.05$). In contrast, IL-1β, IL-6 and IL-18 levels were markedly increased, while IL-10 level were significantly decreased in the miR-22 inhibitor group (all $P < 0.05$). There were no significant differences in IL-1β, IL-6, IL-18 and IL-10 levels between the blank, NC and miR-22 inhibitor + siNLRP3 groups (all $P > 0.05$) (Table 3).

## Discussion

This study explored the effects of miR-22 on the NLRP3 inflammasome in EC injury in CHD. According to results, our study indicated that miR-22 can down-regulate the levels of inflammatory cytokines by suppressing NLRP3 inflammasome activation, which exerts an active role in protecting CAECs.

Typical and mature atherosclerosis plaques were present in the coronary arteries of rats in the atherosclerosis group after oil red-O staining. Atherosclerosis is regarded as

an inflammatory process consisting of high lipid accumulation along the artery wall [19]. Therefore, a CHD model was successfully established in this study with high-fat diets. Compared with the normal group, the TC, TG, and LDLC levels and the concentration of $Ca^{2+}$ were increased in the atherosclerosis group, indicating an increased concentration of serum lipids and blood calcium in rats with CHD. Accumulating evidence has recently proven that the high levels of serum lipids can increase the possibility of CHD [20]. Chi et al. argued that reducing TC, TG and LDLC levels serves as an efficient therapeutic means to treat atherosclerosis [21]. Yu et al. also claimed that CHD can be attenuated by mediating several cardiovascular disease risk factors, such as hypercholesterolemia and hypertension [22]. Kalampogias et al. indicated that calcium mineralization contributed to the solidification of atherosclerotic plaque formation, leading to narrowed arteries [23].

One of our main findings was that miR-22 was negatively associated with NLRP3 and caspase-1 *in vitro* and *in vivo*. MiR-22 was down-regulated in the inflammatory response, which contributed to CHD [13]. NLRP3 is the initial protein in a cascade that leads to inflammasome intracellular activation [24]. Moreover, miRNAs act as significant regulators by inhibiting NLRP3 inflammasome activity [18, 25]. Therefore, it was hypothesized that *NLRP3* was a potential target gene of miR-22, which was further confirmed by the results from the dual-luciferase reporter assays. Caspase-1 activation induced EC dysfunction, leading to vascular remodeling and atherosclerosis [26]. Similarly, Li et al. also demonstrated that miR-20a over-expression reduced the formation of the NLRP3 inflammasome, including reducing NLRP3 and caspase-1 expression [27], which possibly explains how miR-22 expression is related to NLRP3 and caspase-1 in our study.

Another important result is that miR-22 can reduce EC injury in CHD. Senescent injured ECs are related to promoting apoptosis, reducing the proliferation rate and increasing inflammatory proteins [28]. EC injury and senescence are associated with cardiovascular diseases in elderly patients [29]. In this experiment, miR-22 decreased the apoptosis rate and increased cell activities in ECs under CHD stress; these cells also still possessed lumen-forming abilities. It has been shown that miR-22 over-expression can prevent EC injury by mediating apoptosis, the cell survival rate and lumen-forming abilities. In accordance with our results, Tadokoro et al. claimed that certain exogenous miRNAs enhances the lumen-forming abilities in ECs [30]. Ming et al. found that endothelial progenitor cell senescence can be suppressed through a miR-22 pathway, which could in turn promote endothelial progenitor cell proliferation and migration [31].

Atherosclerosis is a chronic inflammatory disease associated with a variety of inflammatory cytokines [32]. In this experiment, the levels of inflammatory cytokines were measured by ELISA. Our results showed that IL-1β, IL-6 and IL-18 levels were down-regulated, and IL-10 levels were up-regulated in the miR-22 mimic group. IL-1β, IL-6 and IL-18 are pro-inflammatory cytokines that are predominantly produced by monocytes or macrophages and control important functions in the immune system as well as inflammatory responses, such as inducing cell differentiation and inhibiting cell growth [33, 34]. IL-18 can promote plaque rupture and myocardial infarction in atherosclerosis and plaque development by increasing cholesterol levels [35]. Sustained IL-6 trans-signaling participates in chronic low-level inflammation, which results in insulin resistance and further contributes to atherosclerosis [36]. High IL-1β secretion plays multiple roles in the formation and stability of atherosclerosis by eliciting the production of other inflammatory molecules secreted by macrophages and ECs [37]. However, IL-10 is considered an important anti-inflammatory cytokine and is known to suppress the formation of atherosclerosis plaques [38].

## Conclusion

Our observations provided evidence that miRNA-22 up-regulation has the great potential to mediate the expression of NLRP3 inflammatory cytokines that protect CAECs. It is believed that therapeutic strategies directed toward restoring miR-22 function would be

helpful in CHD treatment. Nevertheless, the sensitivity and specificity of miR-22 needs to be further examined to confirm the results and clinical value of this microRNA.

## Acknowledgements

This research was supported by National Natural Science Foundation of China (No. 81560046), Guangxi Natural Science Foundation (No. 2016GXNSFAA380002), Promotional Project of Guangxi Medical and Health Appropriate Technology (No.S201518) and Scientific Project of Guangxi Higher Education (No. KY2015ZD028). The authors acknowledge all the reviewers who had given supports for our article.

## Disclosure Statement

None.

## References

1 Sayed AS, Xia K, Li F, Deng X, Salma U, Li T, Deng H, Yang D, Haoyang Z, Yang T, Peng J: The diagnostic value of circulating microRNAs for middle-aged (40-60-year-old) coronary artery disease patients. Clinics (Sao Paulo) 2015;70:257-263.

2 Sotoudeh Anvari M, Mortazavian Babaki M, Boroumand MA, Eslami B, Jalali A, Goodarzynejad H: Relationship between calculated total antioxidant status and atherosclerotic coronary artery disease. Anatol J Cardiol 2016;16:689-695.

3 Braza-Boils A, Mari-Alexandre J, Molina P, Arnau MA, Barcelo-Molina M, Domingo D, Girbes J, Giner J, Martinez-Dolz L, Zorio E: Deregulated hepatic microRNAs underlie the association between non-alcoholic fatty liver disease and coronary artery disease. Liver Int 2016;36:1221-1229.

4 Go AS, Mozaffarian D, Roger VL, Benjamin EJ, Berry JD, Blaha MJ, Dai S, Ford ES, Fox CS, Franco S, Fullerton HJ, Gillespie C, Hailpern SM, Heit JA, Howard VJ, Huffman MD, Judd SE, Kissela BM, Kittner SJ, Lackland DT, Lichtman JH, Lisabeth LD, Mackey RH, Magid DJ, Marcus GM, Marelli A, Matchar DB, McGuire DK, Mohler ER, 3rd, Moy CS, Mussolino ME, Neumar RW, Nichol G, Pandey DK, Paynter NP, Reeves MJ, Sorlie PD, Stein J, Towfighi A, Turan TN, Virani SS, Wong ND, Woo D, Turner MB, American Heart Association Statistics C, Stroke Statistics S: Heart disease and stroke statistics--2014 update: a report from the American Heart Association. Circulation 2014;129:e28-e292.

5 Wu JM, Hsieh TC, Yang CJ, Olson SC: Resveratrol and its metabolites modulate cytokine-mediated induction of eotaxin-1 in human pulmonary artery endothelial cells. Ann N Y Acad Sci 2013;1290:30-36.

6 Iyer S, Chhabra Y, Harvey TJ, Wang R, Chiu HS, Smith AG, Thomas WG, Pennisi DJ, Piper M: CRIM1 is necessary for coronary vascular endothelial cell development and homeostasis. J Mol Histol 2016;10.1007/s10735-016-9702-3

7 Peng Y, Song L, Zhao M, Harmelink C, Debenedittis P, Cui X, Wang Q, Jiao K: Critical roles of miRNA-mediated regulation of TGFbeta signalling during mouse cardiogenesis. Cardiovasc Res 2014;103:258-267.

8 Small EM, Olson EN: Pervasive roles of microRNAs in cardiovascular biology. Nature 2011;469:336-342.

9 Diehl P, Fricke A, Sander L, Stamm J, Bassler N, Htun N, Ziemann M, Helbing T, El-Osta A, Jowett JB, Peter K: Microparticles: major transport vehicles for distinct microRNAs in circulation. Cardiovasc Res 2012;93:633-644.

10 Damavandi Z, Torkashvand S, Vasei M, Soltani BM, Tavallaei M, Mowla SJ: Aberrant Expression of Breast Development-Related MicroRNAs, miR-22, miR-132, and miR-212, in Breast Tumor Tissues. J Breast Cancer 2016;19:148-155.

11 Patel JB, Appaiah HN, Burnett RM, Bhat-Nakshatri P, Wang G, Mehta R, Badve S, Thomson MJ, Hammond S, Steeg P, Liu Y, Nakshatri H: Control of EVI-1 oncogene expression in metastatic breast cancer cells through microRNA miR-22. Oncogene 2011;30:1290-1301.

12 Zuo QF, Cao LY, Yu T, Gong L, Wang LN, Zhao YL, Xiao B, Zou QM: MicroRNA-22 inhibits tumor growth and metastasis in gastric cancer by directly targeting MMP14 and Snail. Cell Death Dis 2015;6:e2000.

13 Chen B, Luo L, Zhu W, Wei X, Li S, Huang Y, Liu M, Lin X: miR-22 contributes to the pathogenesis of patients with coronary artery disease by targeting MCP-1: An observational study. Medicine (Baltimore) 2016;95:e4418.

14 Wang L, Qu P, Zhao J, Chang Y: NLRP3 and downstream cytokine expression elevated in the monocytes of patients with coronary artery disease. Arch Med Sci 2014;10:791-800.

15 He J, Yang Y, Peng DQ: Monosodium urate (MSU) crystals increase gout associated coronary heart disease (CHD) risk through the activation of NLRP3 inflammasome. Int J Cardiol 2012;160:72-73.
16 Huck O, Elkaim R, Davideau JL, Tenenbaum H: Porphyromonas gingivalis-impaired innate immune response via NLRP3 proteolysis in endothelial cells. Innate Immun 2015;21:65-72.
17 Haneklaus M, O'Neill LA, Coll RC: Modulatory mechanisms controlling the NLRP3 inflammasome in inflammation: recent developments. Curr Opin Immunol 2013;25:40-45.
18 Bauernfeind F, Rieger A, Schildberg FA, Knolle PA, Schmid-Burgk JL, Hornung V: NLRP3 inflammasome activity is negatively controlled by miR-223. J Immunol 2012;189:4175-4181.
19 Ma L, Zhong J, Zhao Z, Luo Z, Ma S, Sun J, He H, Zhu T, Liu D, Zhu Z, Tepel M: Activation of TRPV1 reduces vascular lipid accumulation and attenuates atherosclerosis. Cardiovasc Res 2011;92:504-513.
20 Tang K, Lin M, Wu Y, Yan F: Alterations of serum lipid and inflammatory cytokine profiles in patients with coronary heart disease and chronic periodontitis: a pilot study. J Int Med Res 2011;39:238-248.
21 Chi L, Peng L, Hu X, Pan N, Zhang Y: Berberine combined with atorvastatin downregulates LOX1 expression through the ET1 receptor in monocyte/macrophages. Int J Mol Med 2014;34:283-290.
22 Yu D, Zhang X, Gao YT, Li H, Yang G, Huang J, Zheng W, Xiang YB, Shu XO: Fruit and vegetable intake and risk of CHD: results from prospective cohort studies of Chinese adults in Shanghai. Br J Nutr 2014;111:353-362.
23 Kalampogias A, Siasos G, Oikonomou E, Tsalamandris S, Mourouzis K, Tsigkou V, Vavuranakis M, Zografos T, Deftereos S, Stefanadis C, Tousoulis D: Basic Mechanisms in Atherosclerosis: The Role of Calcium. Med Chem 2016;12:103-113.
24 Xiang M, Shi X, Li Y, Xu J, Yin L, Xiao G, Scott MJ, Billiar TR, Wilson MA, Fan J: Hemorrhagic shock activation of NLRP3 inflammasome in lung endothelial cells. J Immunol 2011;187:4809-4817.
25 Fan Z, Lu M, Qiao C, Zhou Y, Ding JH, Hu G: MicroRNA-7 Enhances Subventricular Zone Neurogenesis by Inhibiting NLRP3/Caspase-1 Axis in Adult Neural Stem Cells. Mol Neurobiol 2016;53:7057-7069.
26 Xi H, Zhang Y, Xu Y, Yang WY, Jiang X, Sha X, Cheng X, Wang J, Qin X, Yu J, Ji Y, Yang X, Wang H: Caspase-1 Inflammasome Activation Mediates Homocysteine-Induced Pyrop-Apoptosis in Endothelial Cells. Circ Res 2016;118:1525-1539.
27 Li XF, Shen WW, Sun YY, Li WX, Sun ZH, Liu YH, Zhang L, Huang C, Meng XM, Li J: MicroRNA-20a negatively regulates expression of NLRP3-inflammasome by targeting TXNIP in adjuvant-induced arthritis fibroblast-like synoviocytes. Joint Bone Spine 2016;83:695-700.
28 Rippe C, Blimline M, Magerko KA, Lawson BR, LaRocca TJ, Donato AJ, Seals DR: MicroRNA changes in human arterial endothelial cells with senescence: relation to apoptosis, eNOS and inflammation. Exp Gerontol 2012;47:45-51.
29 Luna C, Alique M, Navalmoral E, Noci MV, Bohorquez-Magro L, Carracedo J, Ramirez R: Aging-associated oxidized albumin promotes cellular senescence and endothelial damage. Clin Interv Aging 2016;11:225-236.
30 Tadokoro H, Umezu T, Ohyashiki K, Hirano T, Ohyashiki JH: Exosomes derived from hypoxic leukemia cells enhance tube formation in endothelial cells. J Biol Chem 2013;288:34343-34351.
31 Ming GF, Wu K, Hu K, Chen Y, Xiao J: NAMPT regulates senescence, proliferation, and migration of endothelial progenitor cells through the SIRT1 AS lncRNA/miR-22/SIRT1 pathway. Biochem Biophys Res Commun 2016;478:1382-1388.
32 Liang X, He M, Chen T, Liu Y, Tian YL, Wu YL, Zhao Y, Shen Y, Yuan ZY: Multiple roles of SOCS proteins: differential expression of SOCS1 and SOCS3 in atherosclerosis. Int J Mol Med 2013;31:1066-1074.
33 Verouti SN, Fragopoulou E, Karantonis HC, Dimitriou AA, Tselepis AD, Antonopoulou S, Nomikos T, Demopoulos CA: PAF effects on MCP-1 and IL-6 secretion in U-937 monocytes in comparison with oxLDL and IL-1beta effects. Atherosclerosis 2011;219:519-525.
34 van de Veerdonk FL, Netea MG, Dinarello CA, Joosten LA: Inflammasome activation and IL-1beta and IL-18 processing during infection. Trends Immunol 2011;32:110-116.
35 Bhat OM, Kumar PU, Giridharan NV, Kaul D, Kumar MJ, Dhawan V: Interleukin-18-induced atherosclerosis involves CD36 and NF-kappaB crosstalk in Apo E-/- mice. J Cardiol 2015;66:28-35.
36 Schuett H, Oestreich R, Waetzig GH, Annema W, Luchtefeld M, Hillmer A, Bavendiek U, von Felden J, Divchev D, Kempf T, Wollert KC, Seegert D, Rose-John S, Tietge UJ, Schieffer B, Grote K: Transsignaling of interleukin-6 crucially contributes to atherosclerosis in mice. Arterioscler Thromb Vasc Biol 2012;32:281-290.
37 Bhaskar V, Yin J, Mirza AM, Phan D, Vanegas S, Issafras H, Michelson K, Hunter JJ, Kantak SS: Monoclonal antibodies targeting IL-1 beta reduce biomarkers of atherosclerosis *in vitro* and inhibit atherosclerotic plaque formation in Apolipoprotein E-deficient mice. Atherosclerosis 2011;216:313-320.
38 Jiang Y, Gao Q, Wang L, Guo C, Zhu F, Wang B, Wang Q, Gao F, Chen Y, Zhang L: Deficiency of programmed cell death 4 results in increased IL-10 expression by macrophages and thereby attenuates atherosclerosis in hyperlipidemic mice. Cell Mol Immunol 2016;13:524-534.